I S A V

Journal of Theoretical and Applied Vibration and Acoustics

journal homepage: http://tava.isav.ir

Disturbance rejection of three-axis gimbal mechanism using PSO-optimized Fuzzy-PID controller

Mohammad Mohammadian[a], Amir Hossein Rabiee[b*]

[a]*Assistant Professor, Department of Computer and Electrical Engineering, Arak University of Technology, Arak, Iran*

[b]*Assistant Professor, Department of Mechanical Engineering, Arak University of Technology, Arak, Iran*

ARTICLE INFO

Article history:
Received 14 February 2020

Received in revised form
5 June 20

Accepted 23 June 2020

Available online 11 July 2020

Keywords:
Three-axis gimbal mechanism,
Stabilization,
Intelligent controller,
Collaborative simulation.

ABSTRACT

This paper covers the application of the Fuzzy-PID controller to stabilize the three-axis gimbal payload orientation with respect to the inertial frame in the presence of platform motion. In this way, the effect of external disturbances induced by the operating environment is greatly reduced, thereby increasing the accuracy of ultimate operation. Three independent controllers are employed to maintain the triple angles of the three-axis gimbal payload at a desired orientation. The Fuzzy-PID controller benefits the typical PID control structure in which the control gains are adaptively computed by a fuzzy inference system. The particle swarm optimization algorithm is also used to calculate the optimal values of input-output scale factors. A co-simulation platform is considered by coupling the PSO-optimized Fuzzy-PID controllers modeled in Matlab/Simulink to the mechanical gimbal model designed in Solidworks and exported to Simulink by using Simscape toolbox, aiming at the calculation of control torque needed for stabilization of gimbal payload. The effectiveness of the proposed controller is examined by simulation of the designed system for various commanded angles in the presence of different disturbances, including sinusoidal disturbances with diverse frequencies and random vibrations. According to the adopted collaborative simulations, it is shown that the utilized control system performs very well in the tracking of the desired angles and also the rejection of the applied perturbations.

* Corresponding author:
E-mail address: rabiee@arakut.ac.ir (A. H.Rabiee)

http://dx.doi.org/10.22064/tava.2021.124105.1162

1. Introduction

Three-axis camera stabilizers have been frequently employed to fix the Line of Sight (LOS) of the optical sensor with respect to the inertial frame in the presence of platform motion. The ability of the stabilizer to reduce the disturbances has a substantial effect on the quality of the image. Therefore, these systems are frequently employed in the film industry. In addition to handheld cameras, inertial stabilized platforms (ISP) are used in many applications such as astronomical telescopes, tracking, and video surveillance systems. These systems should also be able to point the optical sensor to the commanded orientation. The precise stabilization and pointing in ISP systems require that both mechanical mechanism and controller system should be designed carefully.

Traditionally, three separate PID controllers were used for controlling inertially stabilized platforms [1-3]. In the last years, various advanced controllers have been designed to improve the performance of LOS stabilization in inertial stabilized platforms (ISPs). In [4], Robust H∞ controller has been designed for two-axis gimbal based on the combination of mixed sensitivity and model matching problems. Active disturbance rejection controller (ADRC) is proposed to decrease disturbances and nonlinearities in [5-7]. Target tracking of optical sensors mounted on the UAV has been investigated by employing a model predictive control approach [8]. Sliding mode controllers can handle disturbances and have been widely used in inertial stabilization platforms [9-11]. Sliding mode controllers result in high-frequency chattering which is unpleasant, particularly in mechanical systems. All of these methods are based on models. The performance of model-based controllers highly depends on the accuracy of the models. Any deterioration from the nominal model may degrade the performance of the controller considerably. Unfortunately, Cross-coupling and mass imbalance are presented in Three degrees of freedom (3-DOF) mechanisms. These two important factors lead to time-varying nonlinear effects in the ISP models. Therefore, it seems that the appropriate controller for these systems should not rely on an accurate model.

Recently, model free intelligent controller has been proposed for ISP systems. In [12], the model-free fuzzy and ANFIS PID controllers are proposed for controlling ISP systems. However, mass imbalance and cross-coupling are not considered in the performance evaluation process. In [13, 14], a self-tuning fuzzy PID controller is designed in the presence of cross-coupling and asymmetrical mass distribution. However, PID coefficients are recursively tuned , which may lead to poor transient performance. This motivates us to exploit an effective optimization algorithm to find the best controller's gain for minimizing transient errors. Moreover, the proposed method is based on the simulation of a complicated model. ISPs have a lot of civil applications in various fields with special specifications. Any small variation in gimbal design leads to considerable differences in the model. This problem makes the controller and mechanism design procedure so time-consuming and cumbersome. Therefore, it seems reasonable to provide a flexible simulation platform that enables us to produce an accurate computer model of ISP mechanism. This platform can be employed to design a controller with optimized coefficients that minimize the transient and stabilization errors.

The main contribution of the present work is the modeling and control of 3-DoF gimbal control mechanism in the collaborative software framework (Solidworks and Matlab). Using this simulation framework, without the need to obtain the system's mathematical model (which itself is found using simplifying assumptions), one can evaluate the efficacy of various control

strategies. Simscape has been exploited by many industry-leading companies such as ABB, Airbus, and Volvo for modeling and simulating multi-domain physical systems. In fact, models derived based on software such as Simscape by considering physical details are more reliable for simulating closed-loop system and optimizing controller performance. As a secondary contribution, one can mention utilizing a fuzzy-PID controller to control the 3-DoF gimbal mechanism. Accordingly, first, the Solidworks 3D model is designed and then exported to the Simscape Multi-body model in the Simulink environment. The benefit of modeling the gimbal mechanism in this way is that the mass imbalance and cross-couplings can be modeled easily. Moreover, the effect of any modification of the mechanism design on the dynamic model can be studied easily. In Simulink, an actuator can be attached to each joint to apply the required torque. In addition, a sensor can be added to the final payload to measure roll, pitch, and yaw angles. The primary contribution of this paper is to design an optimized fuzzy controller for LOS stabilization of three-axis gimbal. By using particle swarm optimization (PSO) method, Fuzzy PID controller scale factors can be selected such that minimize root mean square (RMS) of the error. PSO algorithm helps us to reduce transient and steady-state error considerably.

This paper is organized as follows: in the methodology section, we introduce CAD assembly designed in Solidworks for 3-DOF mechanism and then export it to Simulink through Simscape. We then show how to connect required actuators and sensors to the mechanical design. Next, we present our method to design an intelligent controller based on fuzzy logic and particle swarm optimization. In simulation results section, we examine controller performance in various aspects, such as transient error, steady-state error, and disturbance rejection. Finally, in conclusion section, we summarize the main points of the article.

2. Methodology

2.1. Mechanical design of three-axis gimbal mechanism

Mathematical models presented in the literature are usually derived based on some simplification assumptions. Therefore, these models are not as accurate as the Simscape model. Moreover, these models depend on the parameters of the system. So, any variation in mechanical design may lead to severe variation in the model. Consequently, in the present study, the Simscape model instead of the mathematical model is proposed. The mechanical design of the multi-link mechanism type gimbal components and the accurate assembly of the parts are necessary to be done first. As mentioned before, the gimbal modeling is executed on the Solidworks platform. The final model of the gimbal assembly is shown in Figure 1. As can be seen in this figure, the gimbal mechanism is composed of several components. Part 1 is the base part of the mechanism that attaches to the main body of the device in question. Links 2 and 3, as well as the payloads (Part 4), are connected by a rotary joint. There are also three electric motors mounted on the rotary joints. Particularly, our aim is to keep the payload stable at the desired angles despite environmental disturbances to the gimbal assembly.

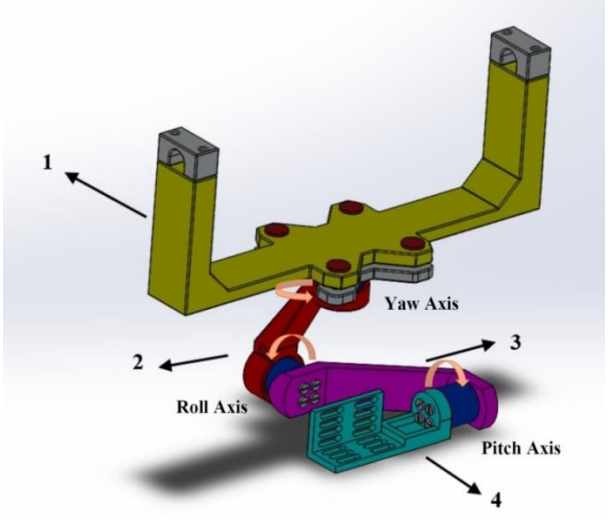

Fig. 1. Designed three-axis gimbal mechanism

Once the gimbal mechanism is modeled, there is a need for simultaneous and online communication between the Solidworks and Matlab/Simulink platforms. To do this, depending on the software version, you will the associated files need to be downloaded from Matlab website and the appropriate guideline should be followed [15]. In this way, the SimMechanics toolbox will be added to the Solidworks platform. Next, the Simulink model of the three-axis gimbal mechanism is generated by the SimMechanics toolbox. The finalized modified Simulink gimbal model for stabilizing the payload orientation, including the body blocks, the disturbance section, the angle calculator, and the control systems, is shown in Figure 2. Here, the Body Sensor and Body Actuator blocks are used to control the body blocks, and the Joint Actuator and Joint Sensor blocks are utilized to control joint blocks that are constrained between components. As mentioned before, the objective of the present study is to stabilize payload angles in inertial coordinates. Therefore, the payload angles of the pitch, roll, and yaw must be measured precisely. In practice, the IMU sensor is used to measure these triple angles. In the present collaborative simulations, the payload-related Body Sensor is adjusted to be the rotational matrix relative to the inertial coordinates. Then, using a simple code, the pitch, roll, and yaw angles are calculated relative to the inertial coordinates. In the next step, each of the measured angles is compared with the desired reference angle and the calculated error signal is sent to the Fuzzy-PID controller. The controller calculates the torque that must be applied to the specific part by utilization of the Joint Actuator block. One of the advantages of the proposed collaborative approach is that by simply moving the gimbal base, the effect of disturbances on the final sensor can be investigated. For this purpose, a gimbal-type joint with three degrees of freedom can be attached to the base body and then, using the Joint Actuator can apply pitch, roll, and yaw angle to the gimbal base part.

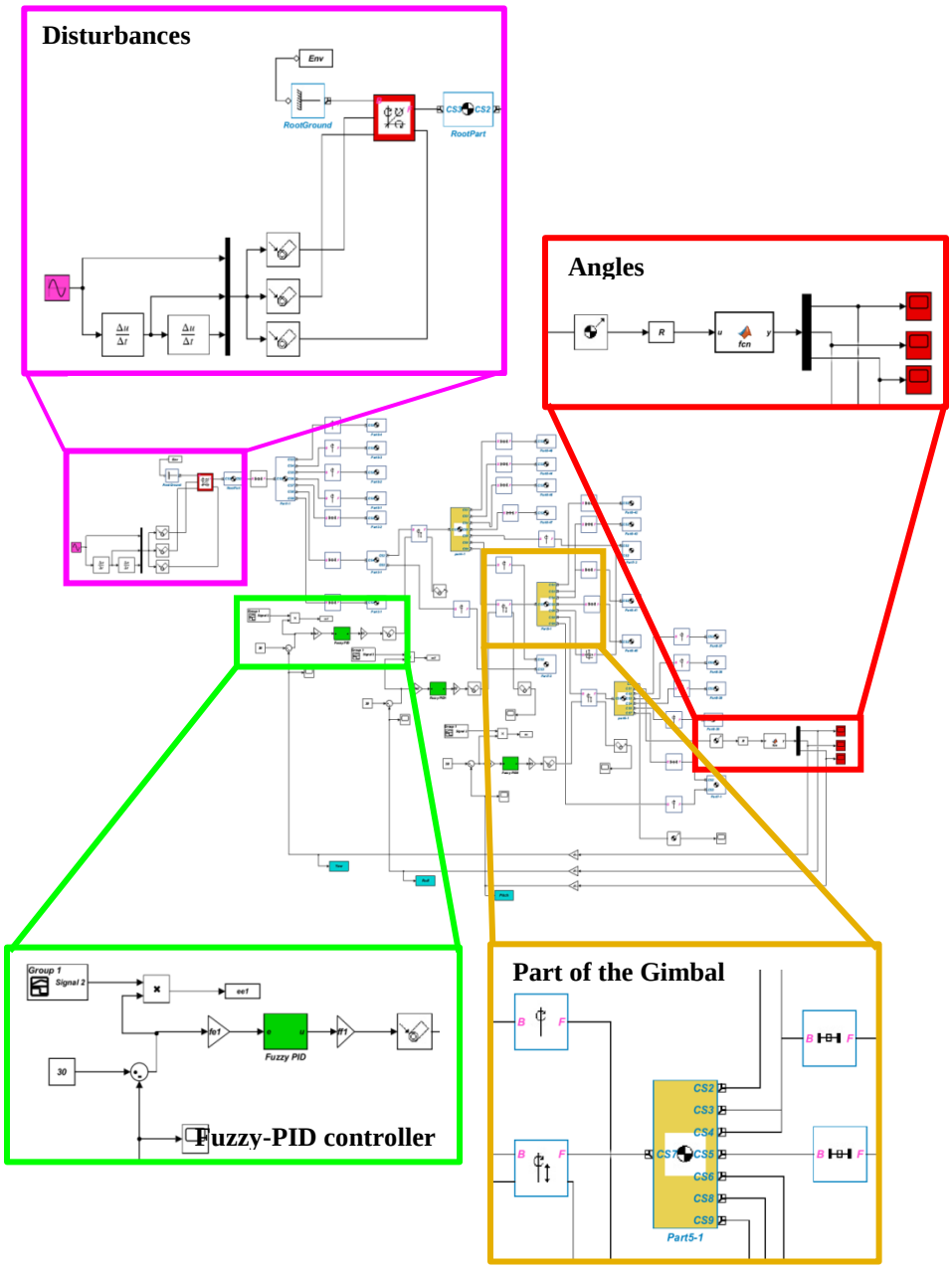

Fig. 2. Finalized Simulink model of three-axis link type gimbal mechanism and associated control system

2.2. Fuzzy-PID controller

In control engineering science, one can find different control strategies, each targeting a specific objective. Since a mathematical model of the plant is not presented in the current study, a model-free controller is the best option to choose. Among such model-free controllers, the fuzzy-PID controller is a well-established one. The main goal of the present paper is to present a collaborative simulation framework for the control mechanism of the gimbal, for which the fuzzy-PID controller is merely one of the many model-free controllers. At its core, there lies a PID controller that is the workhorse of many industries, thanks to its simplicity and great

efficacy. Accordingly, the parameters of PID controller are tuned in an online fashion with the aid of the fuzzy system, thus enhancing the efficiency and adaptability of the control system.

The central core of the fuzzy-PID controller is a classical PID controller in which the ultimate control signal is the sum of three proportional, integral, and derivative parts. In PID controllers, the control gains are generally constant coefficients that are adjusted prior to control action. In the fuzzy-PID controller, the proportional, integral, and derivative gains related to the PID controller are continuously tuned using the fuzzy system during the control action. In fuzzy-PID controllers, the fuzzy part does not directly affect the control signal, i.e., it only sets PID control gains. As observed in Figure 3, PID control inputs, error signal, and its output, are control signals. On the other hand, the error signal and its time derivative enter the fuzzy system. Next, using a fuzzy inference system, the values of proportional, integral, and derivative gains are calculated and applied to the system. The PSO section of this study is a completely independent part with the goal of real-time computation of scale factors. The amplitude or equivalently the power of the control signal depends on the scale factors of the input and output of the fuzzy-PID controller. Here, the PSO algorithm obtains the input and output scale factors in an offline manner (before the start of the control action). In fact, the optimal values of factors are found from the PSO optimization algorithm.

As shown in Figure 3, three independent Fuzzy-PID controllers are employed. In order to design the proper controller, precise mathematical modeling of the system behavior is needed. It is very difficult, if not impossible, to attain a precise mathematical model for complex dynamic systems, for instance, the current three-axis gimbal mechanism. On the other hand, intelligent model-free controllers using numerous intelligent computing methods, such as Bayesian probability, neural network, evolutionary algorithms, fuzzy logic, etc., can estimate the exact control output simply by utilizing the feedback signal and therefore disregard the necessity for an accurate mathematical model of system behavior [16-19]. However, the typical PID control algorithm is widely used in the industry owing to its reliability, simplicity, robustness, and effective practical application [20]. The key internal element of the PID control strategy is proportional constant, which decreases the error but reduces the general stability of the system. Moreover, the integral constant may entirely eradicate the steady-state error for the preferred set point; though, it slows down the system response. On the contrary, the derivative constant improves the performance of the closed-loop system, whereas it can actually increase the noise [21]. Particularly, in recent years, several methods have been proposed for adjusting the PID control gains to obtain better performance according to the expected control goals, including settling time, steady-state error, overshoot, rise time, etc. Many of the aforementioned tuning techniques, called offline methods, the PID control parameters are selected optimally predetermined and then are held constant during the system operation. Conversely, in the online tuning techniques, the PID control parameters are continuously adjusted throughout the system operation by using parameter estimation approaches. Therefore, the controller keeps its performance, mainly owing to its ability to adapt to diverse and unexpected operational situations. Newly, a fuzzy inference system has been used to adaptively adjust PID gains according to some information of the system behavior [22]. Consequently, the fuzzy-PID controller can be considered as a model-free controller in which proportional, derivative and integral gains can be adjusted online according to the error value and the corresponding time derivative. Thereafter, the typical PID control law is considered as [22]:

$$T_{\mathrm{A}} = K_{\mathrm{P}}\, e(t) + K_{\mathrm{I}} \int_0^t e(\tau)\mathrm{d}\tau + K_{\mathrm{D}}\, \dot{e}(t), \tag{1}$$

where T_{A} is control torque applied to each of the three rotational joints. In addition, the error signal is written as

$$e(t) = \theta_{\mathrm{d}}(t) - \theta(t), \tag{2}$$

where $\theta_{\mathrm{d}}(t)$ is the desired angle, the proportional and derivative control parameters $(K_{\mathrm{P}}, K_{\mathrm{D}})$ are assumed to remain in the predefined ranges of $[K_{\mathrm{P}}^{\min}, K_{\mathrm{P}}^{\max}]$ and $[K_{\mathrm{D}}^{\min}, K_{\mathrm{D}}^{\max}]$, respectively. In the next step, the proportional and derivative gains should be normalized as follows:

$$K_{\mathrm{P}}^{'} = (K_{\mathrm{P}} - K_{\mathrm{P}}^{\min}) / (K_{\mathrm{P}}^{\max} - K_{\mathrm{P}}^{\min}) \tag{3}$$

$$K_{\mathrm{D}}^{'} = (K_{\mathrm{D}} - K_{\mathrm{D}}^{\min}) / (K_{\mathrm{D}}^{\max} - K_{\mathrm{D}}^{\min}) \tag{4}$$

Also the integral control parameter K_{I} is defined as

$$K_{\mathrm{I}} = K_{\mathrm{P}}^2 / (\alpha K_{\mathrm{D}}) \tag{5}$$

The integral parameter α, with the normalized control parameters ($K_{\mathrm{P}}^{'}$, $K_{\mathrm{D}}^{'}$) are adjusted via the fuzzy inference system, which is simply installed on a conventional PID control strategy. The following paragraph briefly presents a general scenario for designing fuzzy gain scheduling and tuning the PID control system properly. At first, the input signals $(e, \dot{e})$ are fuzzified to fuzzy sets as following: negative big, negative medium, negative small, zero, positive small, positive medium, and positive big. Additionally, the output signals ($K_{\mathrm{P}}^{'}$, $K_{\mathrm{D}}^{'}$, α) are fuzzified to some fuzzy sets as small, medium-small, medium, and big. The appropriate ranges of input and output signals and their associated membership functions are displayed in Fig. 4. After that, the proper if-then rules are defined as listed in Table 1. Lastly, the outputs are attained according to the Mamdani inference method and the actual (crisp) value associated with $K_{\mathrm{P}}^{'}$, $K_{\mathrm{D}}^{'}$, and α are acquired by aid of center of gravity (COG) defuzzification technique. The proportional, integral, and derivative control parameters $(K_{\mathrm{P}}, K_{\mathrm{D}}, K_{\mathrm{I}})$ are re-computed based on Eqs. (3)-(5).

In this article, the coefficients of the PID controller are considered time-dependent parameters. This makes the stability evaluation and determination of the stability margin a challenging problem. Accordingly, to avoid large transient responses, a supervisory system can be designed to monitor the behavior of the control system. It is preferable to diagnose the instability in the preliminary stages. Once instability is detected over the monitor period, the next correcting steps are taken. Such steps include, but are not limited to, disabling the control system by setting K_{P} to zero or changing control parameters to predefined stabilizing ones to assure the prolonged system stability.

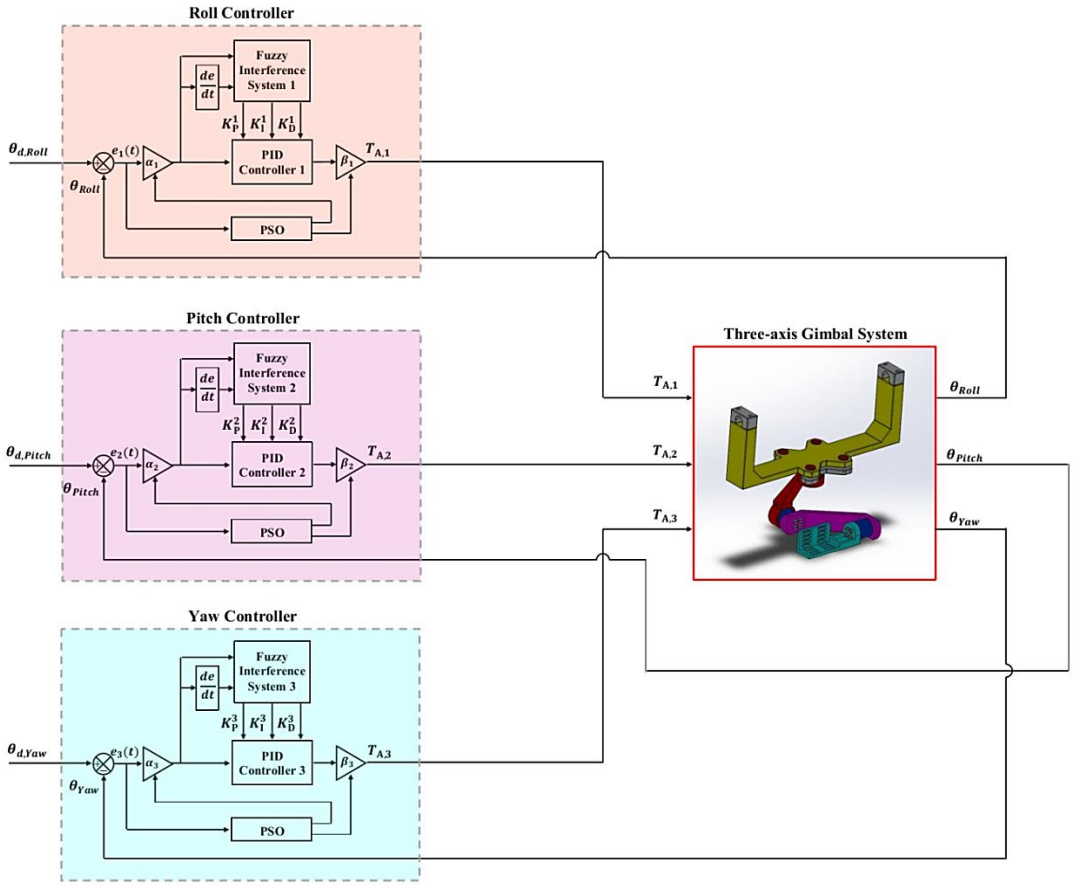

Fig. 3. The general block diagrams of utilized control systems for stabilizing gimbal mechanism

Table 1: Utilized Fuzzy if-then rules

e	**d*e*** / **d*t***						
	NB	NM	NS	ZO	PS	PM	PB
NB	B/S/S	B/S/S	B/S/S	B/S/S	B/S/S	B/S/S	B/S/S
NM	S/B/MS	M/B/MS	M/M/S	M/M/S	M/M/S	M/B/MS	S/B/ MS
NS	S/B/M	S/B/MS	M/B/MS	M/M/S	M/B/MS	S/B/MS	S/B/M
ZO	S/B/B	S/B/M	S/B/MS	M/B/MS	S/B/MS	S/B/M	S/B/B
PS	S/B/M	S/B/MS	M/B/MS	M/M/S	M/B/MS	S/B/MS	S/B/M
PM	S/B/MS	M/B/MS	M/M/S	M/M/S	M/M/S	M/B/MS	S/B/MS
PB	B/S/S	B/S/S	B/S/S	B/S/S	B/S/S	B/S/S	B/S/S

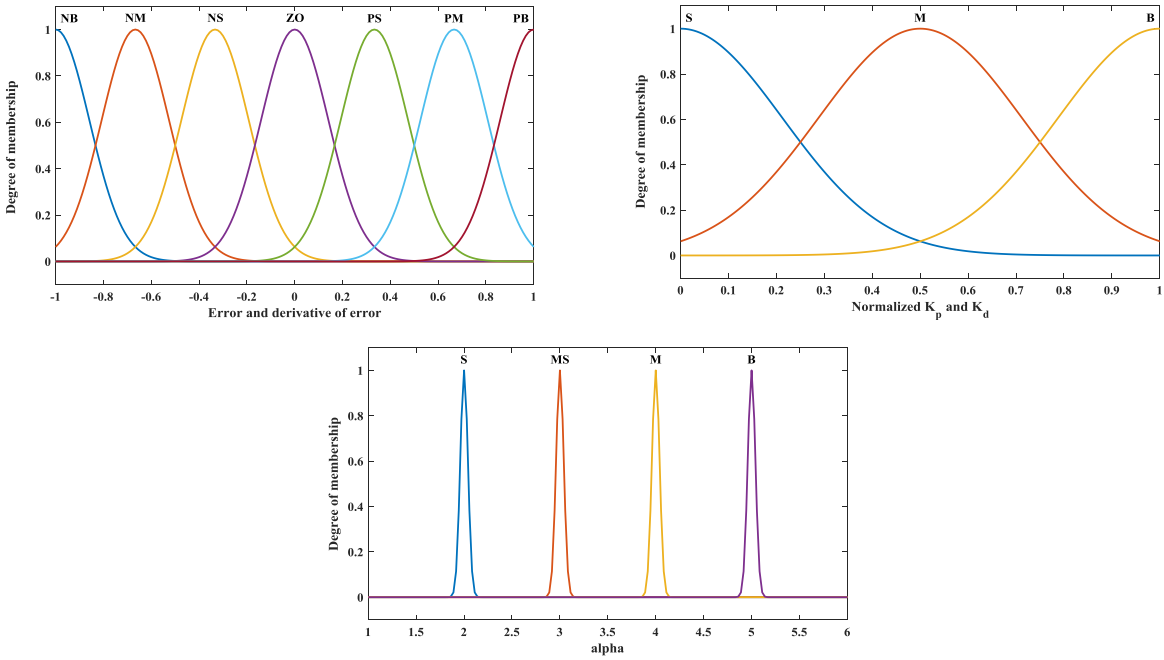

Fig. 4. Fuzzy membership functions for present Fuzzy-PID controller

2.3. Particle swarm optimization

If the objective is to optimize the parameters of fuzzy sets and fuzzy if-then rules, the optimization problem becomes too complex, making access to the final optimal controller more difficult. In the current article, as well as other studies [23-25], a uniform distribution of fuzzy sets over the universe of fuzzy controllers is taken, and the optimization is carried out for only scale factors. In fact, the authors did their best to find a reasonable compromise between the performance and simplicity of the control structure. To this aim, they only considered the optimization of scale factors that directly affect the control signal amplitude. The offline optimization approach is considered and implemented by employing Particle swarm optimization (PSO) algorithm. Particle swarm optimization (PSO) algorithm is considered as a comparatively efficient and new metaheuristic optimization algorithm founded on swarm intelligence. This kind of artificial computing approach is designed by the local influence of group members or the group among themselves and the interaction between particles. Particle swarm optimization, was introduced by Kennedy and Eberhart in 1995 [26], performs exceptionally well in various optimization tasks. PSO algorithm begins the process of solving the problem with a group of different particles. There are two "best" values, which are updated during the optimization process; one of them is the most proper solution that the particle has reached so far, titled P_{best}. The second best value is the most appropriate one, which is between the entire optimization domain and between all the particles. Since the second-best value is identified, it is titled G_{best}. The motion and position of all particles change continuously alongside two directions. Each of the particles has a tendency to move toward the best position that the same particle has taken till at the moment, and the other particle tendency is to move toward the best position of all particles. Suppose that the solution to a specific problem in a D-dimensional domain utilizing PSO algorithm. In particular, the position and the velocity of t D-dimensional vectors $x_i = [x_{i1}, x_{i2}, \dots, x_{iD}]^T$ and $v_i = [v_{i1}, v_{i2}, \dots, v_{iD}]$. In addition, the best-known particle position

(P_{best}) is currently defined as $p_i = [p_{i1}, p_{i2}, \dots, p_{iD}]^T$. Then, the velocity and the position of the other particles are derived as:

$$v_{id}^{n+1} = c_0\left[w v_{id}^{n} + c_1 r_1^n (p_{id}^n - x_{id}^n) + c_2 r_2^n \left(p_{gd}^n - x_{id}^n\right)\right] \tag{6}$$

$$x_{id}^{n+1} = x_{id}^n + v_{id}^{n+1} \tag{7}$$

in which the g index signifies the particle that has the best position so far among all other particles, the n index represents the echoes, N is the number of algorithm particles, $d = 1, 2, 3, \dots, D$ and $i = 1, 2, 3, \dots, N$, and the constants r_1 and r_2 are random values in the range of $(0, 1)$. The coefficients of r_1 and r_2 permit the particles to move with different step values among P_{best} and G_{best}. When the values of these constants are close to zero, the movement in different directions is limited, while the values approach unity creates more diversity.

Additionally, the c_0, c_1, and c_2 are constant values larger than zero, called acceleration constants, and are normally supposed in the range $(0, 2)$. The closer these constants are to unity, the more restriction in the algorithm explorations and the higher the rate of convergence. Conversely, values close to zero provide better exploration in a specific region. The coefficient w is the inertia weight, which affects convergence in the PSO. The inertia weight controls the effect of previous particles' velocities on present speeds. Consequently, this coefficient can affect the ability of the algorithm to find a proper solution throughout the optimization domain. Obviously, over time, the particles move gradually towards the optimal positions, which increases the tendency of the particles to search nearby the solutions and limits the search space.

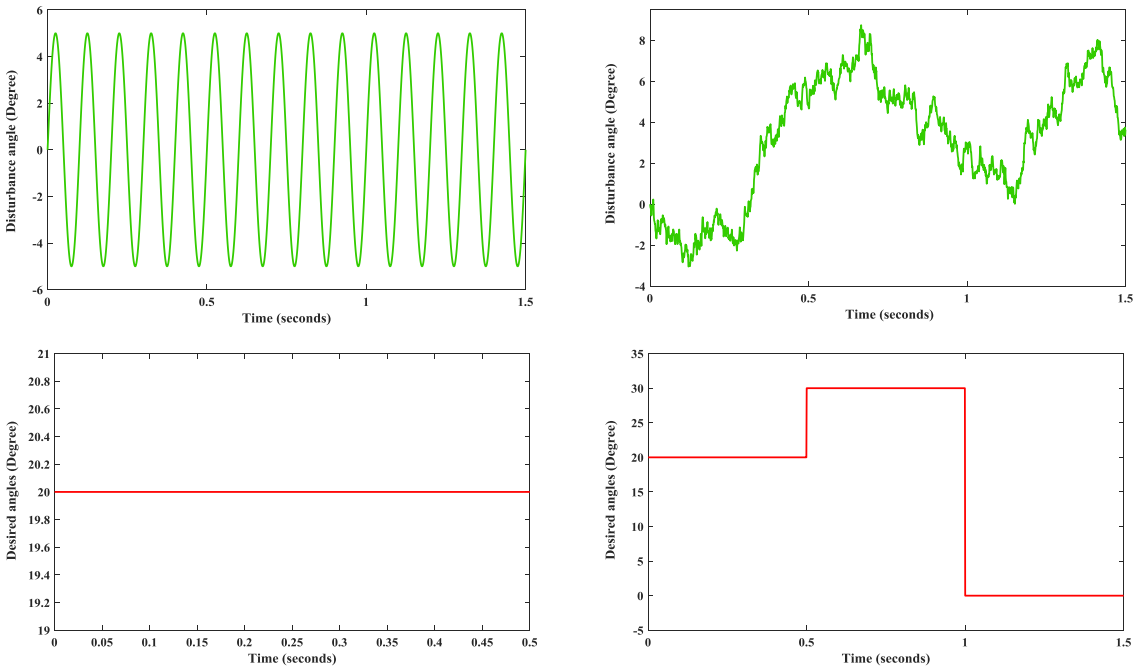

Fig. 5. Utilized applied disturbances and desired reference angles

3. Simulations results

In this section, the key results of collaborative simulations for the stabilization of the payload orientation at the desired angles by the PSO-optimized Fuzzy-PID controller are discussed. To evaluate the performance of the proposed control system, the desired angles of the roll, pitch, and yaw are considered in two constant and stepwise cases. Also, it is assumed that the perturbations are applied to the gimbal in the two oscillating and random conditions; both are illustrated in Fig 5. As stated earlier, in order to obtain the optimal performance of the Fuzzy-PID controller, the scale factor coefficients are taken into account, which are shown in Fig. 3. Consequently, according to the utilization of three independent controllers to stabilize the gimbal orientation, there will be a total of 6 scale factor constants. By utilization of PSO algorithm with the parameters listed in table 2, The coefficients are optimally obtained as $(\alpha_1, \alpha_2, \alpha_3, \beta_1, \beta_2, \beta_3) = (6.5, 6.3, 1.1, 1.8, 1.5, 1.9)$. It is also worth noting that the cost function is considered as $J = [w_1 \max(e_{ss}) + w_2 RMS(e_{ss})]$ intended to perform the optimization process. The cost function is obtained as 39.1 for the final optimal case. The optimization process is performed for constant desired angles and oscillatory perturbation with amplitude 0.5° and frequency 20Hz. Following are the results of collaborative simulations in selected cases by employing the optimized Fuzzy-PID controller, which was designed previously.

Figure 6 shows the time histories of the pitch, roll and yaw angles of payload as well as the Fuzzy-PID control gains during the control action for desirable constant angles $(\theta_{\mathrm{d,Pitch}}, \theta_{\mathrm{d,Roll}}, \theta_{\mathrm{d,Yaw}}) = (20^{\circ}, 20^{\circ}, 20^{\circ})$ and oscillatory perturbations with amplitude 0.5° and frequency 20 Hz. Also, in the same figure, the root mean square (RMS) values of the steady-state error for each of the pitch, roll, and yaw angles are presented. As can be seen from the second row of Fig. 6, the control system performs very well in the tracking of the desired angles and also the rejection of the applied perturbations. Also, the RMS error values for all three angles are approximately 0.08, indicating the effectiveness of the utilized control system.

To analyze the control signals, Figure 7 shows the time history of the control signals associated with Figure 6, which are the torques applied to rotate the mechanism links. It can be seen that at the beginning of the control action, more torque is needed to bring the payload to the desired angles. It can also be seen that the torque required to rotate the payload at angles yaw and roll is higher than that of pitch angle. In addition, in order to evaluate the improvement of the controller performance benefiting the particle swarm optimization algorithm, Figure 8 shows a comparison between the time histories of the pitch, roll, and yaw angles of payload for the Fuzzy-PID controller with and without the PSO algorithm. Here, the efficiency of adjusting the controller parameters using the optimization algorithm is appropriately obvious.

Next, in order to evaluate the effectiveness of the designed controller, the amplitude and frequency of the oscillating disturbances are changed. For this purpose, Figures 9-14 illustrate the diagrams similar to Fig. 6 for oscillatory perturbations with different amplitudes and frequencies. By comparing the figures presented, it can be seen that the designed Fuzzy-PID controller keeps its performance for a wide range of applied disturbances.

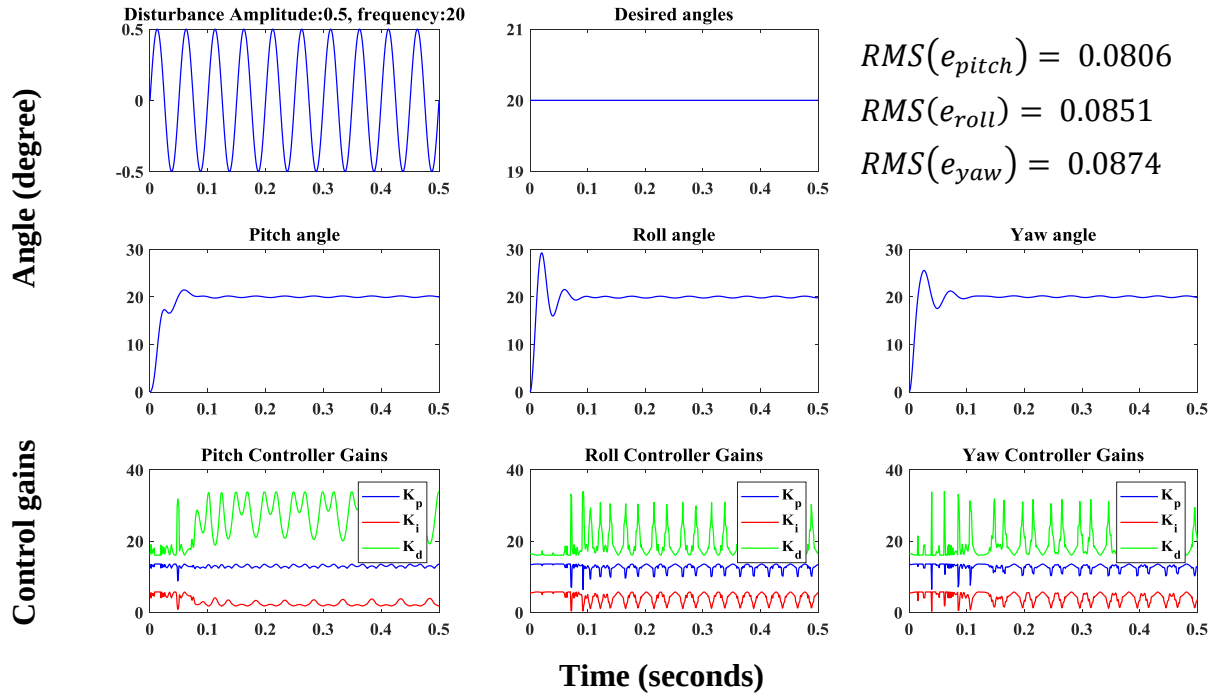

Fig. 6. Time evolutions of the pitch, roll, and yaw angles and Fuzzy-PID control gains for desirable constant angles and oscillatory perturbations with amplitude 0.5° and frequency 20Hz**.**

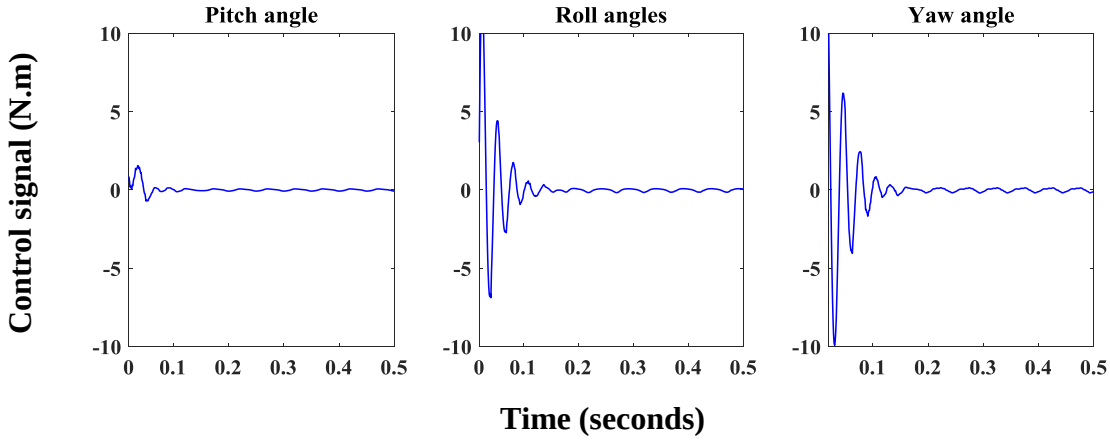

Fig. 7. Time evolutions of the control signals associated with oscillatory perturbations with amplitude 0.5° and frequency 20Hz**.**

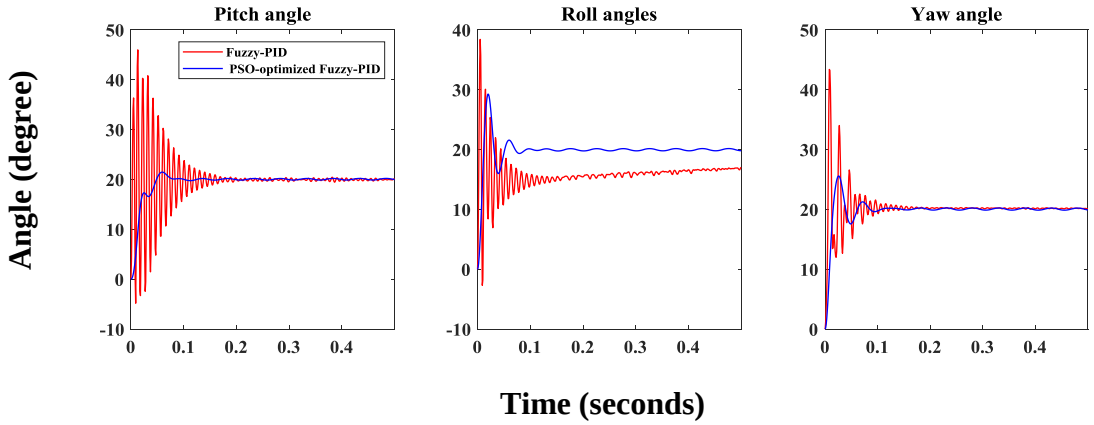

Fig. 8. Time evolutions of the pitch, roll, and yaw angles for Fuzzy-PID controllers with and without optimization algorithm

Table 2. PSO parameters

N	n	w	c_0	c_1	c_2
50	100	0.8	1	2	2

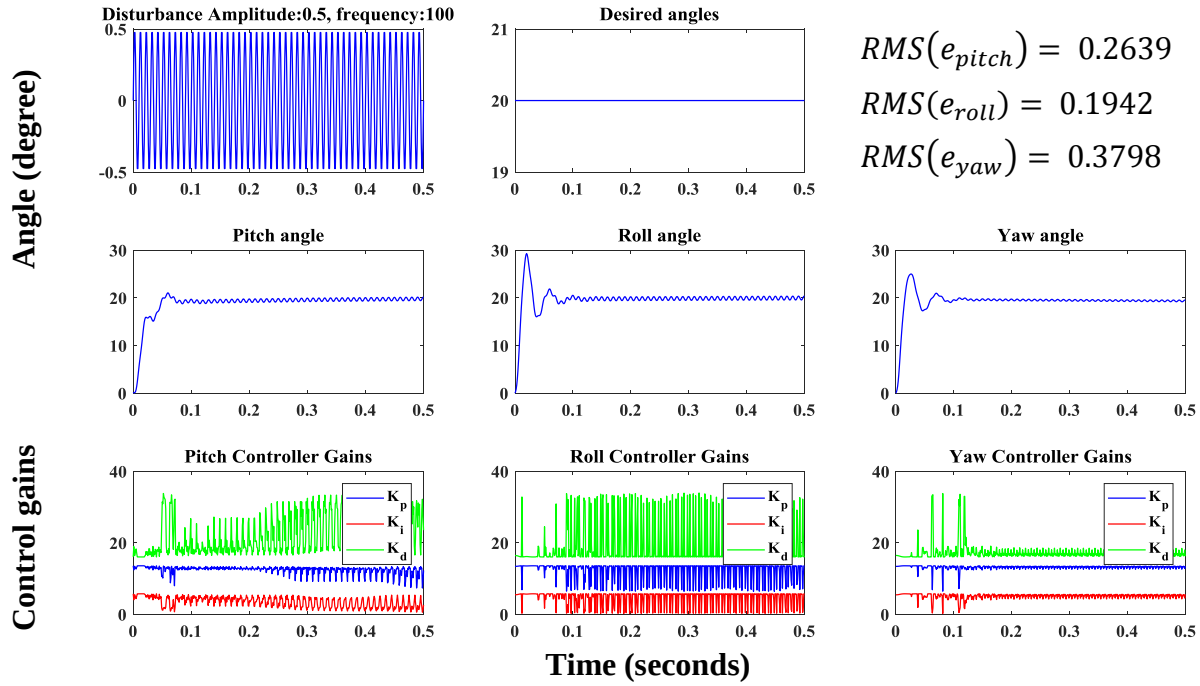

Fig. 9. Time evolutions of the pitch, roll, and yaw angles and Fuzzy-PID control gains for desirable constant angles and oscillatory perturbations with amplitude 0.5° and frequency 100Hz.

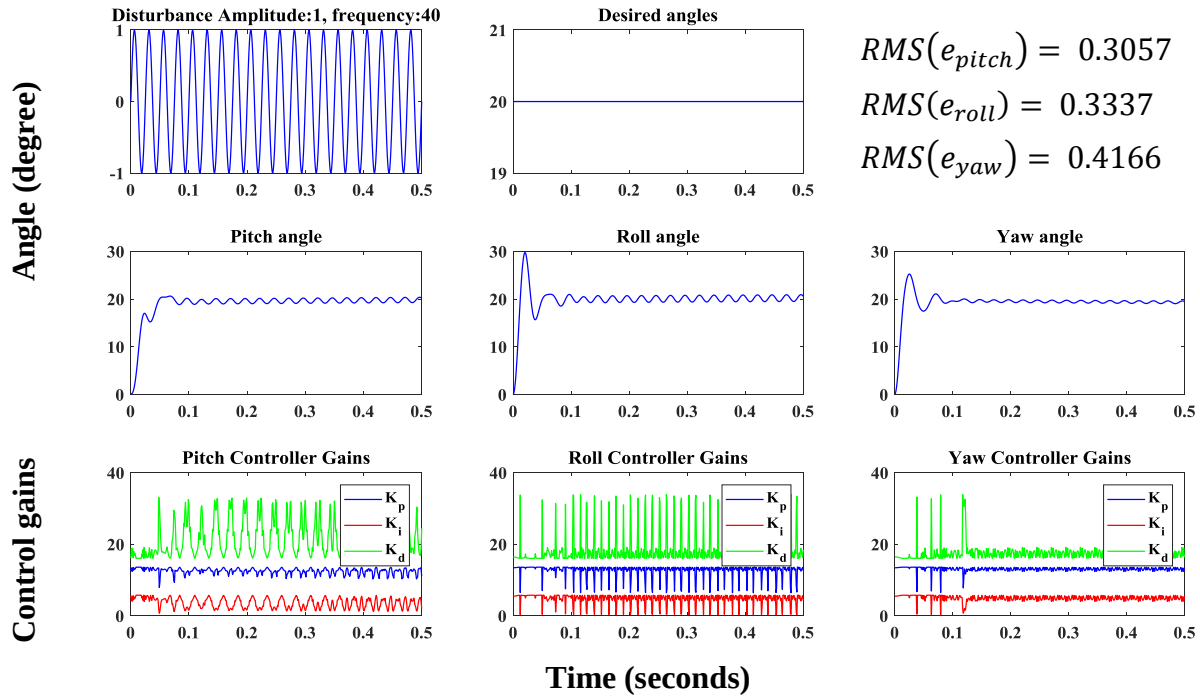

Fig. 10. Time evolutions of the pitch, roll, and yaw angles and Fuzzy-PID control gains for desirable constant angles and oscillatory perturbations with amplitude 1° and frequency 40Hz.

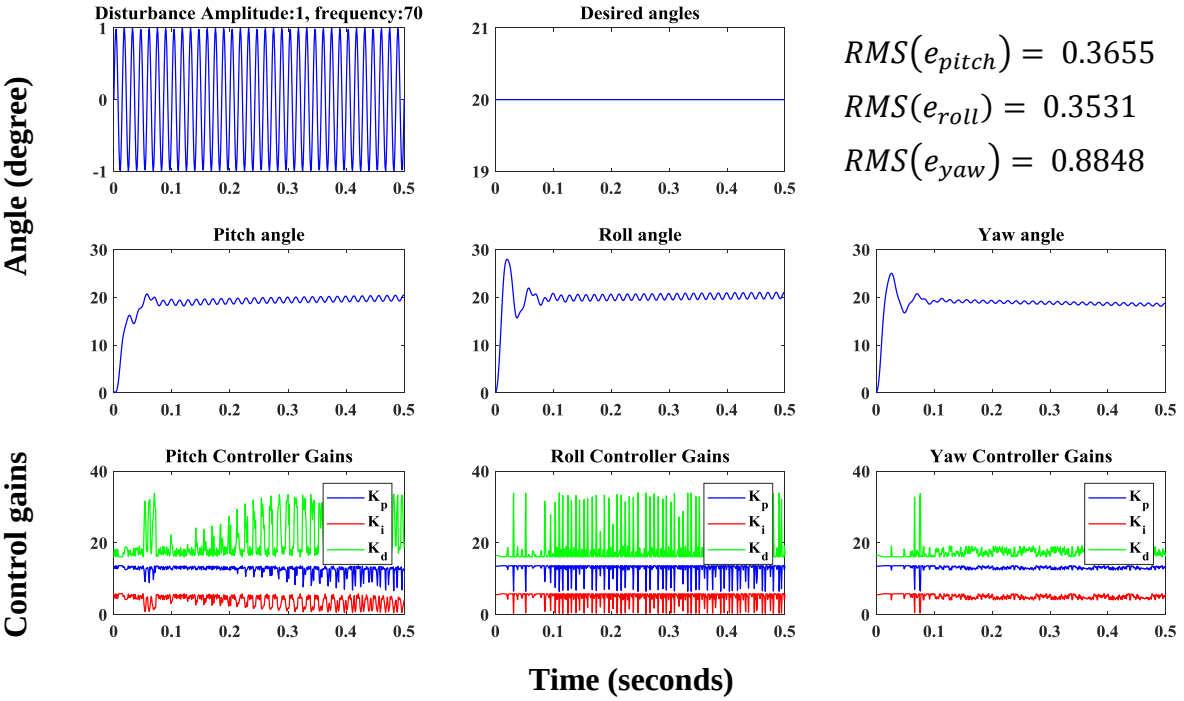

Fig. 11. Time evolutions of the pitch, roll, and yaw angles and Fuzzy-PID control gains for desirable constant angles and oscillatory perturbations with amplitude 1° and frequency 70Hz**.**

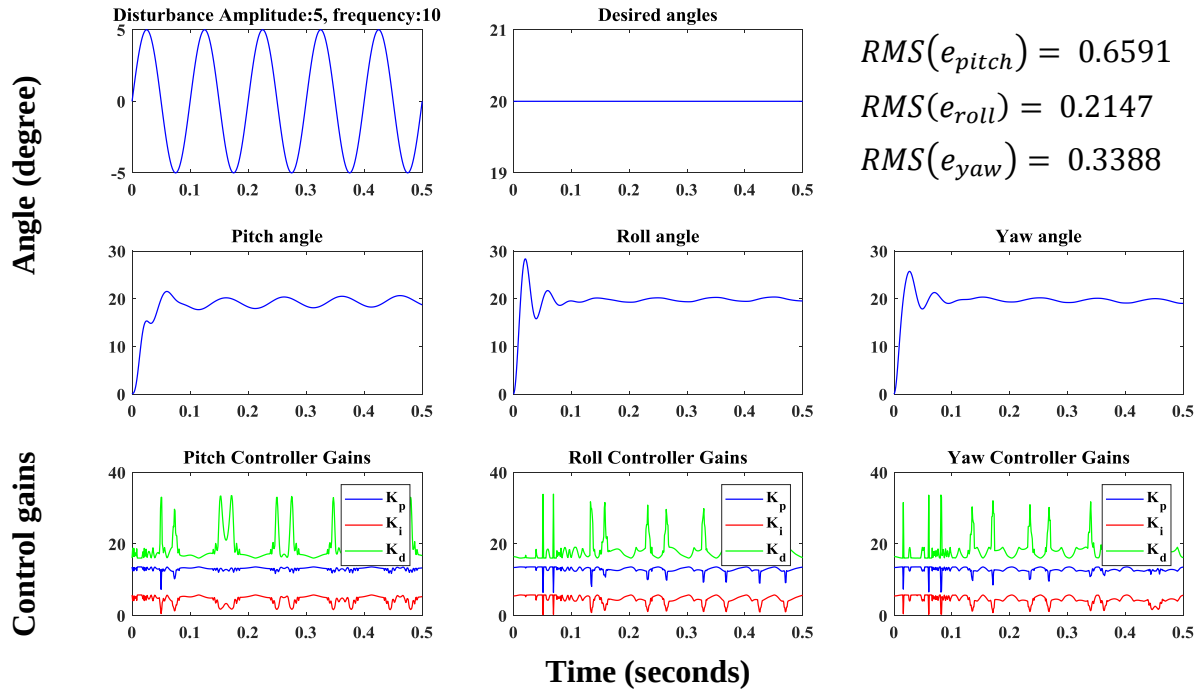

Fig. 12. Time evolutions of the pitch, roll, and yaw angles and Fuzzy-PID control gains for desirable constant angles and oscillatory perturbations with amplitude 5° and frequency 10Hz**.**

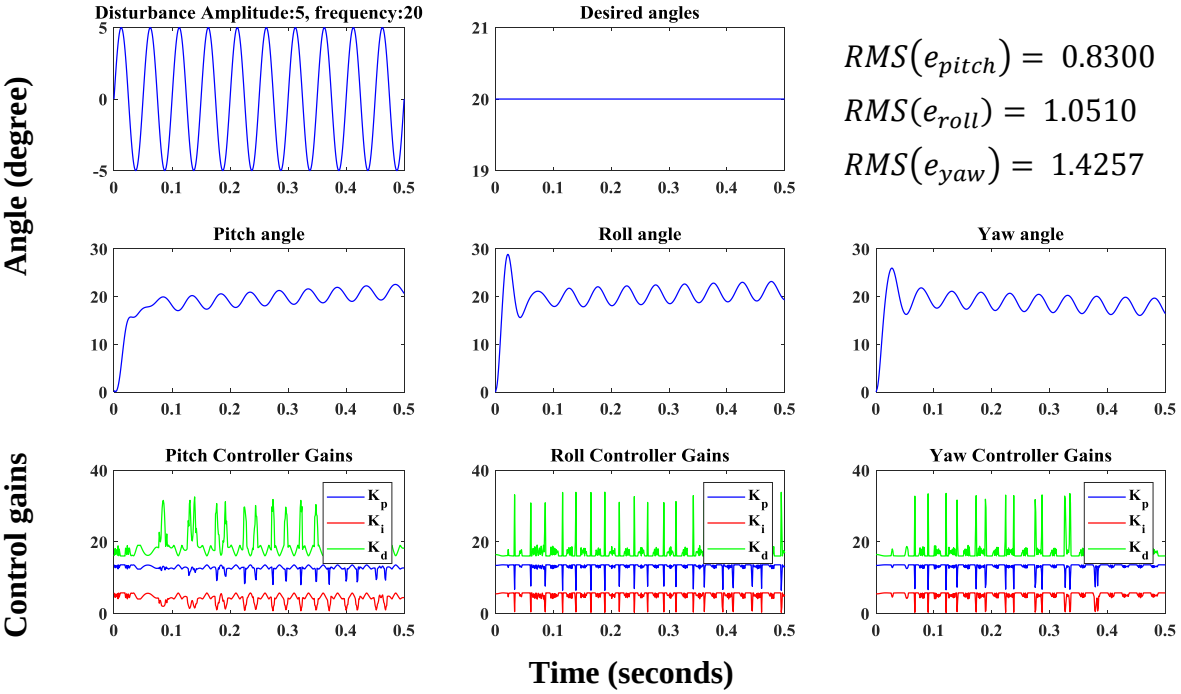

Fig. 13. Time evolutions of the pitch, roll, and yaw angles and Fuzzy-PID control gains for desirable constant angles and oscillatory perturbations with amplitude 5° and frequency 20Hz**.**

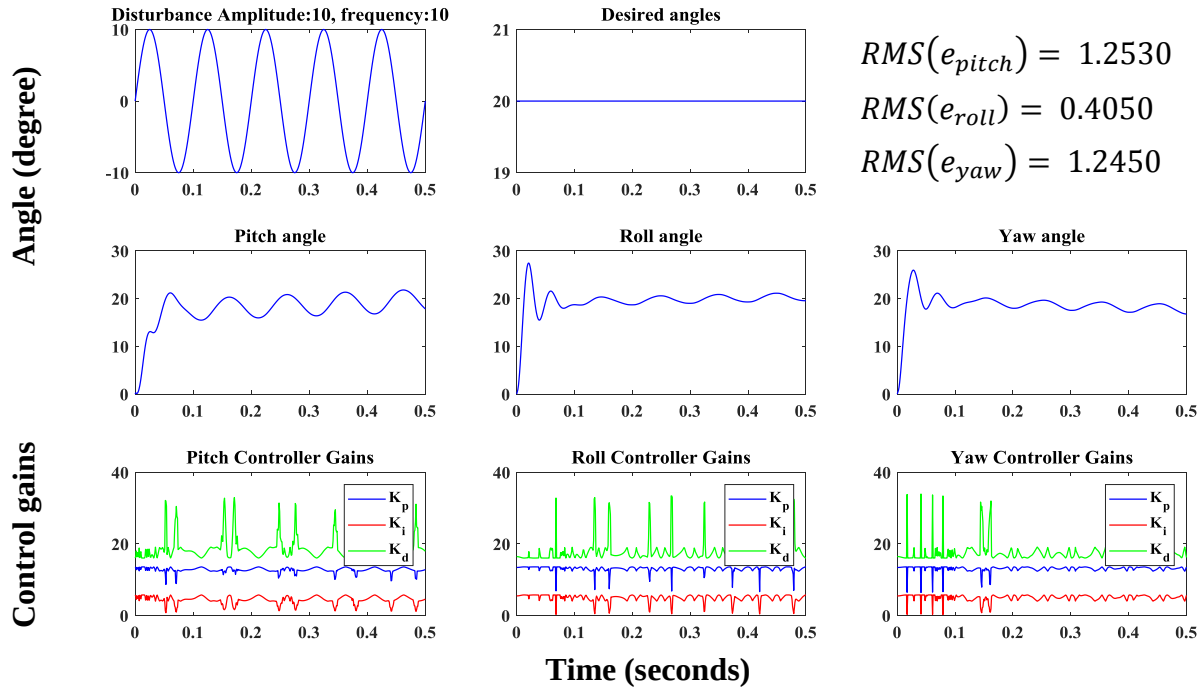

Fig. 14. Time evolutions of the pitch, roll, and yaw angles and Fuzzy-PID control gains for desirable constant angles and oscillatory perturbations with amplitude 10° and frequency 10Hz**.**

As observed in Fig. 9, with the increase of the oscillating disturbance frequencies from 20Hz to 100Hz, the RMS errors of the closed-loop systems have been tripled on average but are still small in comparison with the desired angles. Also, the variation of Fuzzy-PID controller gains increases with an increase in disturbance frequency. Further, with increasing the amplitude of perturbation, it is observed that the magnitude of the payload fluctuations increases. In general, increasing the amplitude and frequency of the oscillating perturbation increases the error signal, although it seems that the effect of the frequency on the error is greater. In addition, it seems the roll angle error is the lowest and the yaw is the highest one among the error values given in all oscillatory disturbances cases. Here, the oscillatory perturbation with amplitude 5° and frequency 20Hz leads to the greatest error. In this case, the pitch, roll, and yaw RMS error values are respectively 10, 12 and, 16 times greater compared to that of the first case (Fig. 6), Whereas the amplitude and frequency of perturbation are 10 and 1 fold, respectively. To better illustrate the effectiveness of the optimized Fuzzy-PID controller as well as highlight the benefits of utilized collaborative simulation, an animation clip for the functionality of the multi-link type gimbal (case of Fig. 8) is posted at [24].

Next, the effectiveness of the proposed Fuzzy-PID controller for a condition where the desired angles change stepwise is presented. For this purpose, Figures 16-19 show the time histories of the pitch, roll, and yaw angles of the payload as well as the Fuzzy-PID control gains during the control action for desirable stepwise angles and oscillatory perturbations with different amplitudes and frequencies. The corresponding results are relatively similar to those obtained previously. It is observed that the intended Fuzzy-PID controller has been able to track the desired payload angles and also reject the effects of applied perturbations. Here again, RMS error values increase by increasing amplitude and frequency of oscillatory disturbances. The greatest

errors belong to the oscillatory perturbation with amplitude 5° and frequency 20Hz, in which the pitch, roll and yaw RMS error values are respectively 42, 6 and, 19 times compared to that of the base case (Fig. 16). In addition, compared to the case where the desired angles were constant, the error rate generally increased. For example, for an oscillatory disturbance with amplitude 10° and frequency 10Hz, the RMS values of pitch, roll, and yaw are 1.63, 3.8, and 1.46 times compared to that of the constant reference angles, respectively. There is also here the recently posted animated clip for the operation of the gimbal mechanism at [25] (case of Fig. 17).

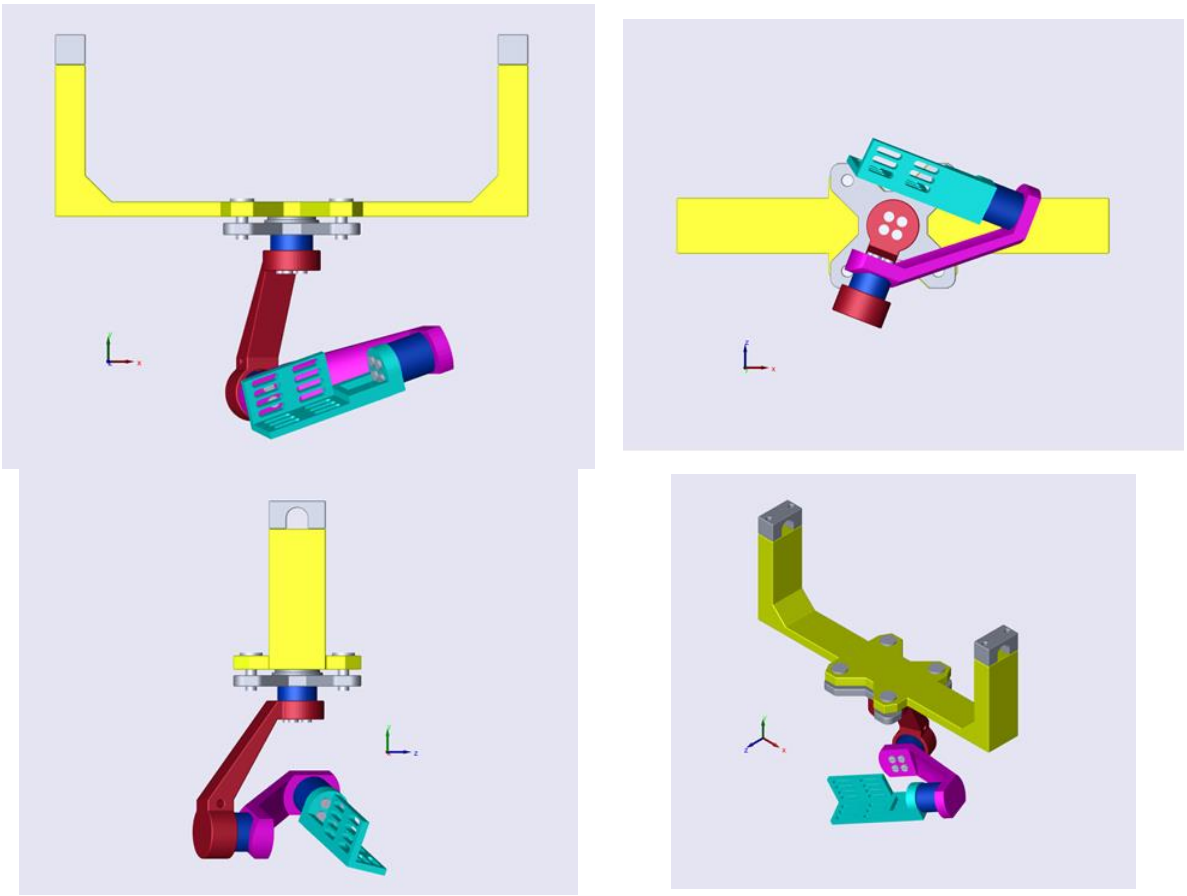

Fig. 15. Stabilized gimbal mechanism for constant desire angles in different views

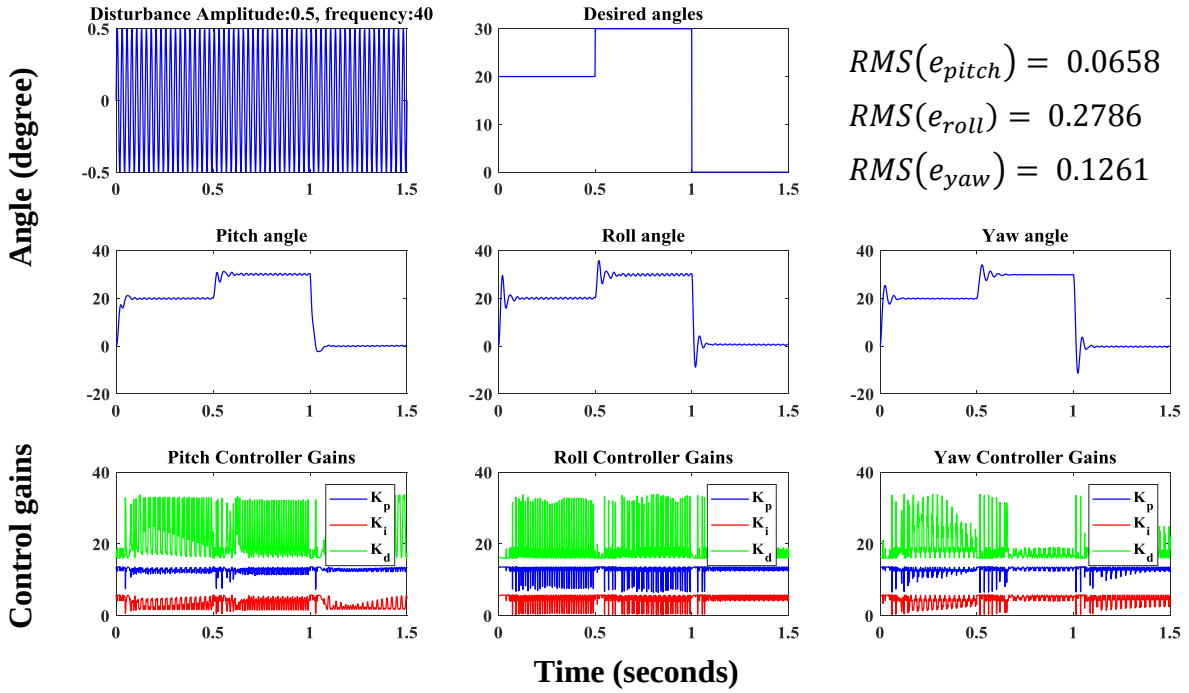

Fig. 16. Time evolutions of the pitch, roll, and yaw angles and Fuzzy-PID control gains for desirable stepwise angles and oscillatory perturbations with amplitude 0.5° and frequency 40Hz**.**

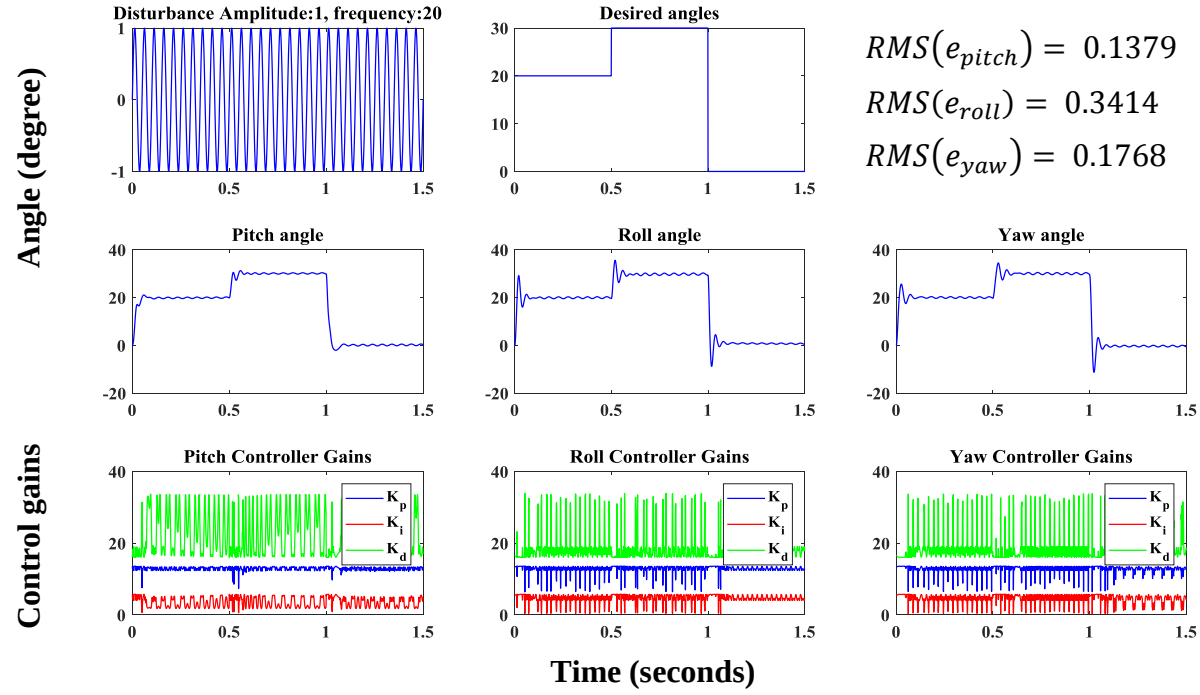

Fig. 17. Time evolutions of the pitch, roll, and yaw angles and Fuzzy-PID control gains for desirable stepwise angles and oscillatory perturbations with amplitude 1° and frequency 20Hz**.**

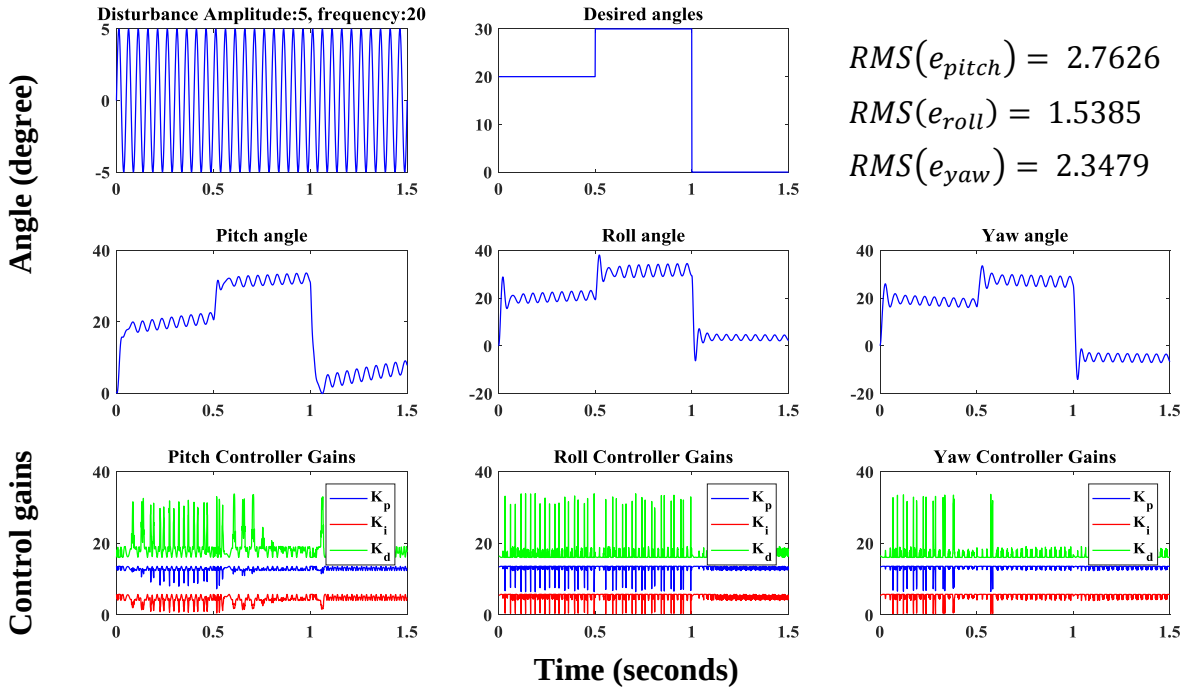

Fig. 18. Time evolutions of the pitch, roll, and yaw angles and Fuzzy-PID control gains for desirable stepwise angles and oscillatory perturbations with amplitude 5° and frequency 20Hz**.**

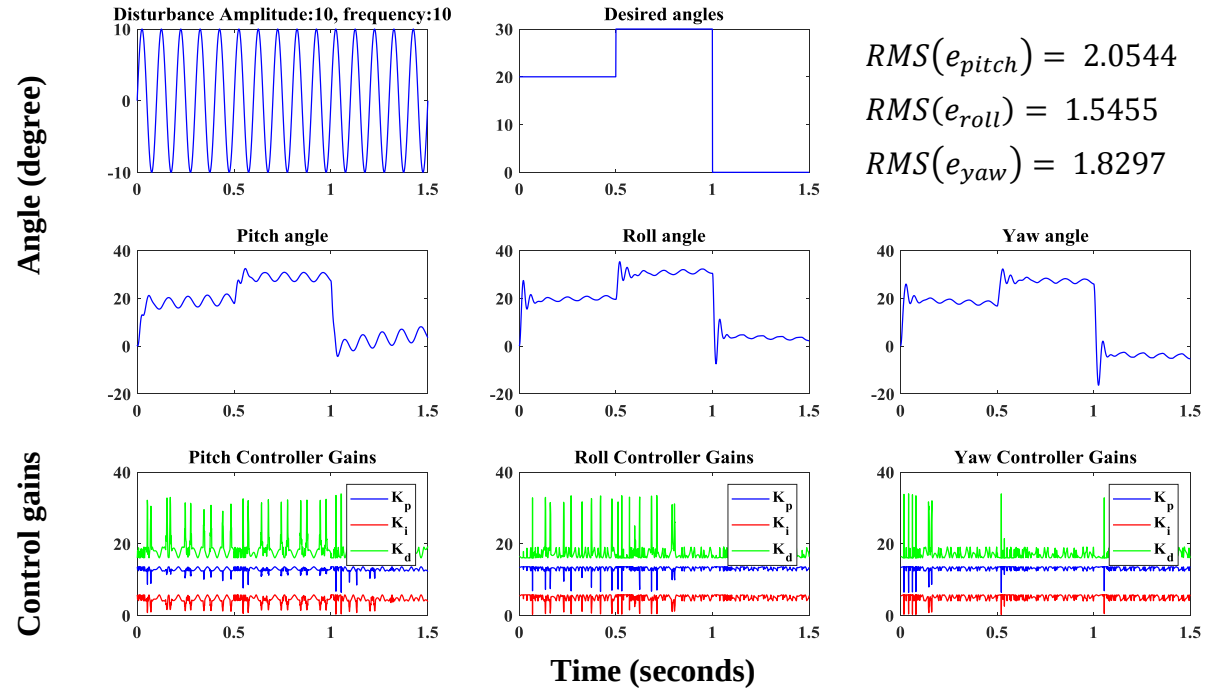

Fig. 19. Time evolutions of the pitch, roll, and yaw angles and Fuzzy-PID control gains for desirable stepwise angles and oscillatory perturbations with amplitude 10° and frequency 10Hz**.**

Finally, the effectiveness of the designed optimized Fuzzy-PID controller for the situation where the gimbal base is subjected to random disturbances is presented**.** For this purpose, Figs. 20-22 show the time histories of the pitch, roll, and yaw angles of the payload during the control action for desirable stepwise angles in the presence of random disturbances with different amplitudes. Here as before, the effectiveness of the controller in the tracking of the desired angles as well as the disturbance rejection is well observed**.** Generally, as the amplitude of the random disturbances increases, an increase in payload fluctuation amplitude is detected. For example, with a 5-fold increase in the random vibration amplitude, the RMS values of the pitch, roll, and yaw angles are 25, 0.8, and 6.5, times greater compared to that of the first case (Fig. 20), respectively, while the same values for the 4-fold increases are 19, 5.5, and 7. There is also here the recently posted animated clip for the operation of the gimbal mechanism at [26] (case of fig. 21).

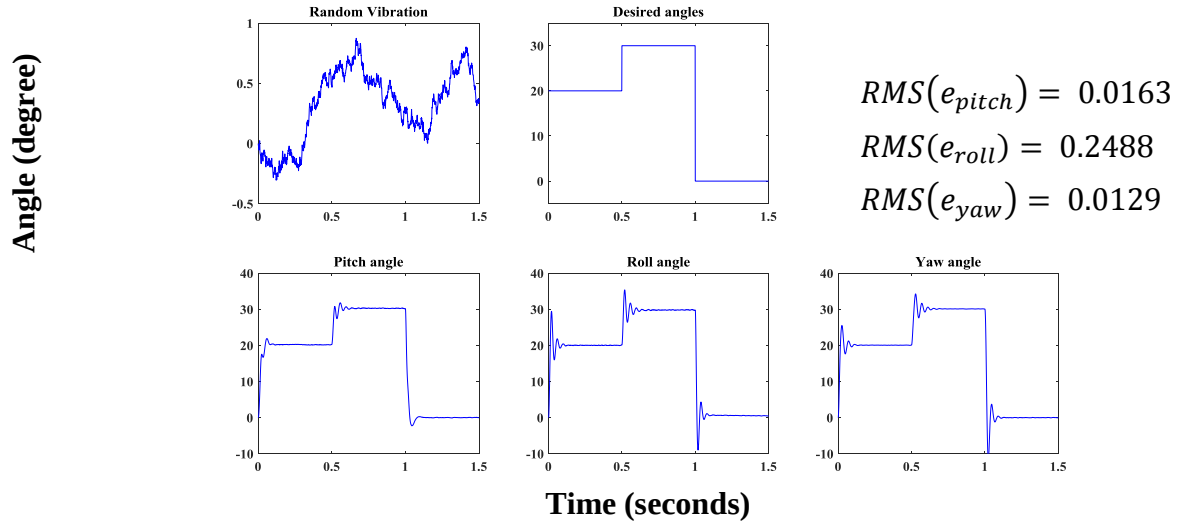

Fig. 20. Time evolutions of the pitch, roll, and yaw angles for desirable stepwise angles and random perturbations with amplitude (case 1)

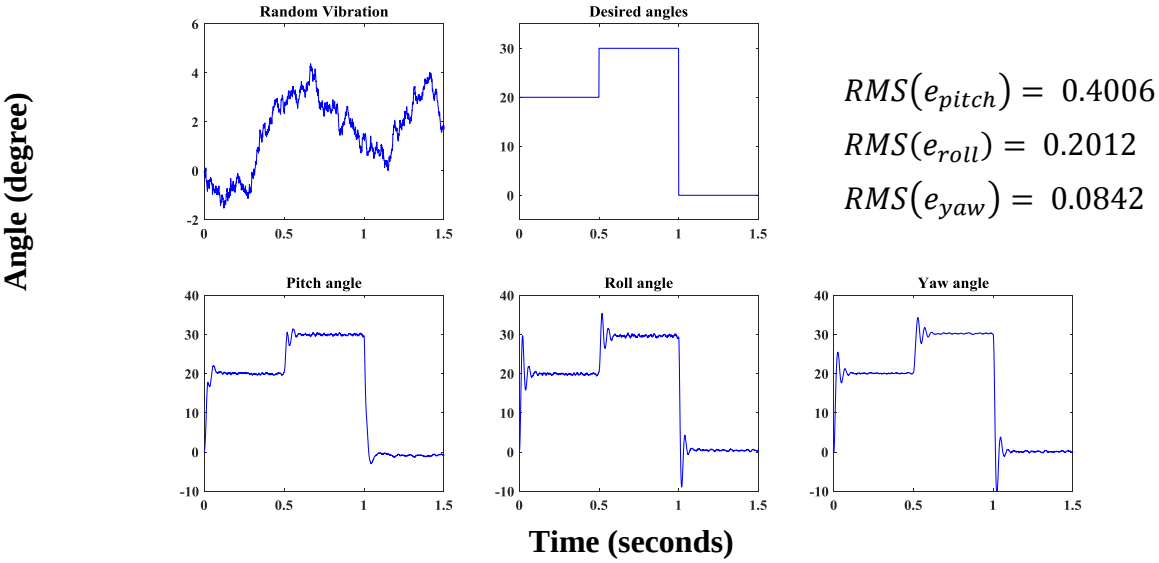

Fig. 21. Time evolutions of the pitch, roll and yaw angles for desirable stepwise angles and random perturbations with amplitude (case 2)

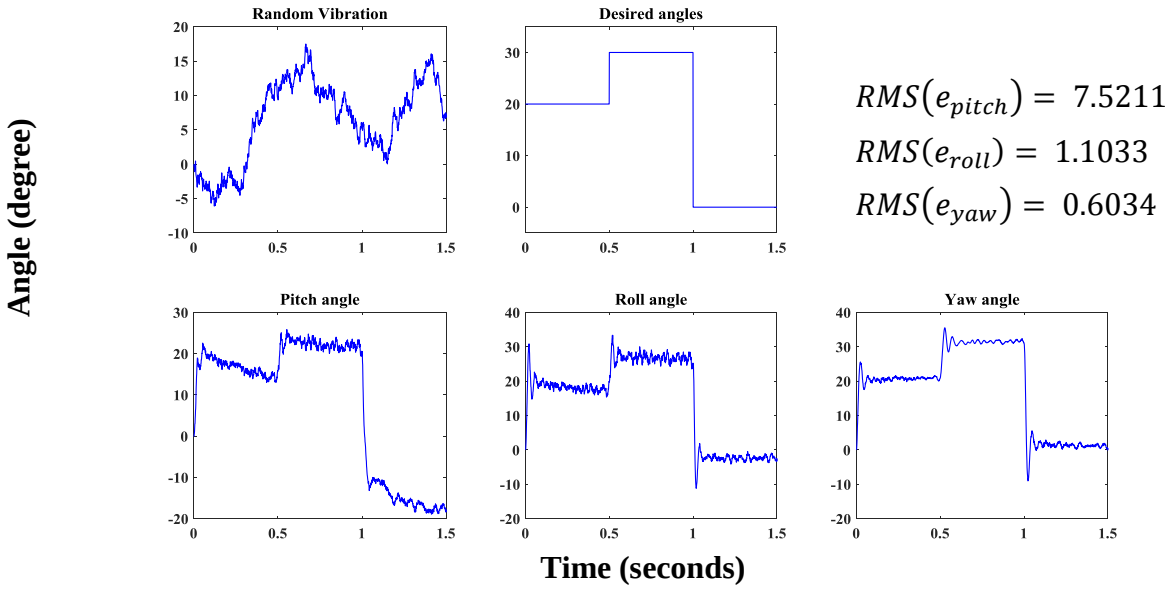

Fig. 22. Time evolutions of the pitch, roll, and yaw angles for desirable stepwise angles and random perturbations with amplitude (case 3)

One of the applications of the gimbal mechanism is to track reference signals other than the step input. Thus, new simulations are conducted to examine its performance with regard to tracking harmonic signals. To this end, Figure 23 shows the roll, pitch, and yaw angles of the gimbal for sinusoidal inputs. In the first to third rows of Figure 23, only one input is taken as sinusoidal, while in the fourth row, all three inputs are sinusoidal. As observed, the fuzzy-PID controller successfully tracks the sinusoidal input to the gimbal mechanism.

4. Conclusions and future works

This paper has developed a new method to design an optimized controller for the inertial stabilization of optical sensors against base vibration and unwanted movement. In addressing this problem, a co-simulation platform is considered by integrating the Fuzzy-PID controller implemented in Simulink/MATLAB and a 3-DOF mechanism designed in Solidworks and exported to Simulink by using Simscape toolbox. It has also been shown that the proposed method has some distinct benefits. First, the detailed mechanical model, including cross-coupling and mass asymmetry, can be derived easily. Next, joint actuators and sensors can be simply attached to the model owing to Simscape. The last and the most important aspect is that it enables us to use the Fuzzy-PID controller in which the controller gains are adaptively computed by a fuzzy inference system and controller scale factors are selected by particle swarm optimization to attain an efficient controller with minimized errors. In the simulation section, we implement the proposed algorithm for a 3-DOF handheld camera stabilizer designed by Solidworks. Controller's scale factors are chosen by means of PSO such that minimizes the tracking error in the presence of sinusoidal disturbances. Finally, the effectiveness of the proposed controller is examined by simulation of the designed system for various commanded angles in the presence of different disturbances, including sinusoidal disturbances with diverse

frequencies and random vibrations. According to the adopted collaborative simulations, it is shown that the utilized control system performs very well in the tracking of the desired angles and also the rejection of the applied perturbations.

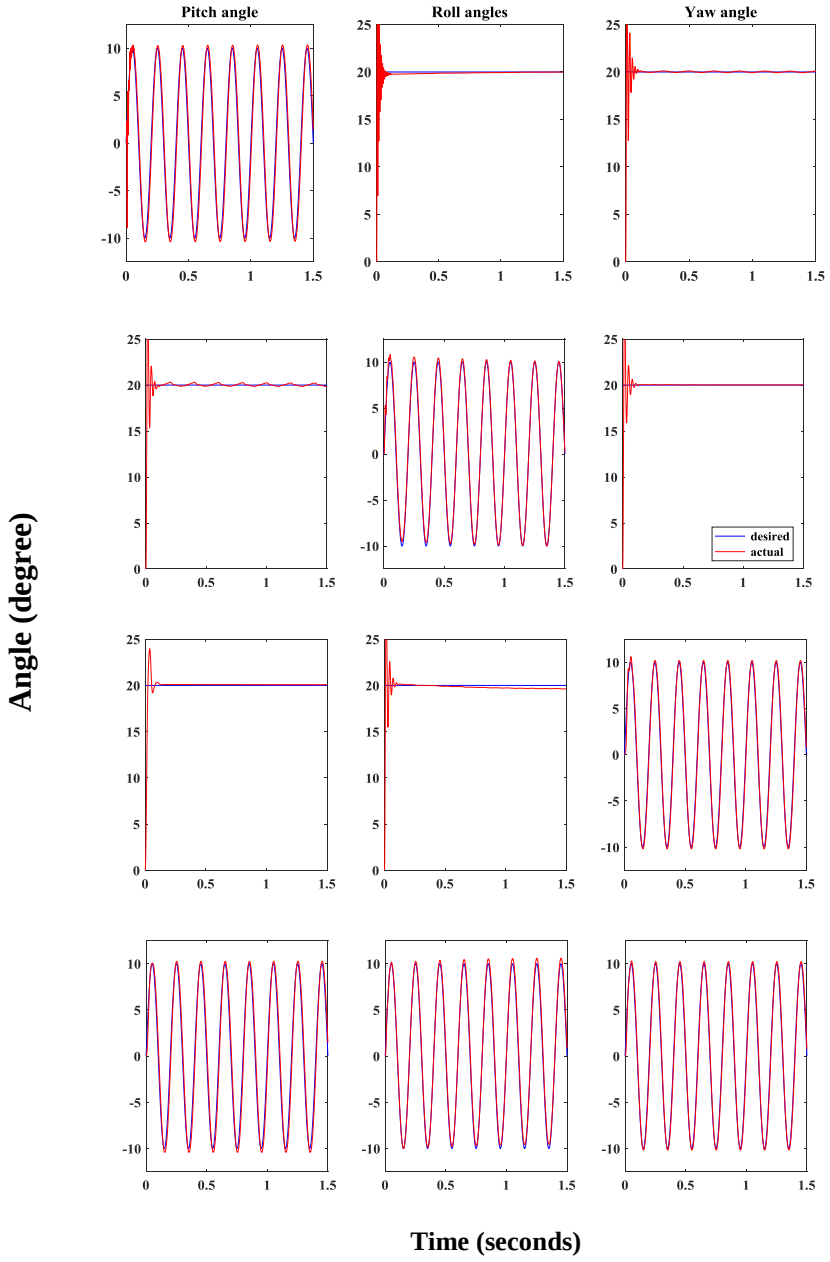

Fig. 23. Time evolutions of the pitch, roll, and yaw angles for desirable Sinusoidal angles

In real applications, electrical motors are utilized to provide the required torque. Designing controller by considering brushless or brushed DC motors can be proposed for future works. Moreover, Takagi-Sugeno Fuzzy controllers that guarantee the stability of the closed-loop system can be considered in the following researches.

References

[1] J. Hilkert, Inertially stabilized platform technology concepts and principles, IEEE control systems magazine, 28 (2008) 26-46.

[2] M.K. Masten, Inertially stabilized platforms for optical imaging systems, IEEE Control Systems Magazine, 28 (2008) 47-64.

[3] P.J. Kennedy, R.L. Kennedy, Direct versus indirect line of sight (LOS) stabilization, IEEE Transactions on control systems technology, 11 (2003) 3-15.

[4] S. Kim, S. Kim, Y. Kwak, Robust control for a two-axis gimbaled sensor system with multivariable feedback systems, IET control theory & applications, 4 (2010) 539-551.

[5] B. Ahi, A. Nobakhti, Hardware implementation of an ADRC controller on a gimbal mechanism, IEEE Transactions on Control Systems Technology, 26 (2017) 2268-2275.

[6] W. Ren, Q. Qiao, K. Nie, Y. Mao, Robust DOBC for Stabilization Loop of a Two-Axes Gimbal System, IEEE Access, 7 (2019) 110554-110562.

[7] F. Wang, R. Wang, E. Liu, W. Zhang, Stabilization Control Mothed for Two-Axis Inertially Stabilized Platform Based on Active Disturbance Rejection Control With Noise Reduction Disturbance Observer, IEEE Access, 7 (2019) 99521-99529.

[8] A. Altan, R. Hacıoğlu, Model predictive control of three-axis gimbal system mounted on UAV for real-time target tracking under external disturbances, Mechanical Systems and Signal Processing, 138 (2020) 106548.

[9] Y.B. Shtessel, Decentralized sliding mode control in three-axis inertial platforms, Journal of Guidance, Control, and Dynamics, 18 (1995) 773-781.

[10] F. Dong, X. Lei, W. Chou, A dynamic model and control method for a two-axis inertially stabilized platform, IEEE Transactions on Industrial Electronics, 64 (2016) 432-439.

[11] J. Mao, J. Yang, X. Liu, S. Li, Q. Li, Modeling and Robust Continuous TSM Control for an Inertially Stabilized Platform With Couplings, IEEE Transactions on Control Systems Technology, (2019).

[12] F. Liu, H. Wang, Q. Shi, H. Wang, M. Zhang, H. Zhao, Comparison of an ANFIS and fuzzy PID control model for performance in a two-axis inertial stabilized platform, IEEE Access, 5 (2017) 12951-12962.

[13] M.M. Abdo, A.R. Vali, A.R. Toloei, M.R. Arvan, Stabilization loop of a two axes gimbal system using self-tuning PID type fuzzy controller, ISA transactions, 53 (2014) 591-602.

[14] G. Sun, X. Wu, Z. Zhong, A self-tuning fuzzy-PID stabilization experiment of a seeker inertial platform's tracking loop subject to input saturation and dead-zone, in: 2016 IEEE International Conference on Aircraft Utility Systems (AUS), IEEE, 2016, pp. 580-585.

[15] G. Hummer, J.C. Rasaiah, J.P. Noworyta, Water conduction through the hydrophobic channel of a carbon nanotube, Nature, 414 (2001) 188-190.

[16] S.M. Hasheminejad, A.H. Rabiee, H. Bahrami, Active closed-loop vortex-induced vibration control of an elastically mounted circular cylinder at low Reynolds number using feedback rotary oscillations, Acta Mechanica, 229 (2018) 231-250.

[17] A.H. Rabiee, Regenerative semi-active vortex-induced vibration control of elastic circular cylinder considering the effects of capacitance value and control parameters, Journal of Mechanical Science and Technology, 32 (2018) 5583-5595.

[18] A.H. Rabiee, Galloping and VIV control of square-section cylinder utilizing direct opposing smart control force, Journal of Theoretical and Applied Vibration and Acoustics, 5 (2019) 69-84.

[19] A.H. Rabiee, M. Esmaeili, Simultaneous vortex-and wake-induced vibration suppression of tandem-arranged circular cylinders using active feedback control system, Journal of Sound and Vibration, (2019) 115131.

[20] S.M. Hasheminejad, A.H. Rabiee, A. Markazi, Dual-Functional Electromagnetic Energy Harvesting and Vortex-Induced Vibration Control of an Elastically Mounted Circular Cylinder, Journal of Engineering Mechanics, 144 (2017) 04017184.

[21] C. Killian, Modern Control Technology: Components and Systems, Thompson Delmar, 2005.

[22] Z.-Y. Zhao, M. Tomizuka, S. Isaka, Fuzzy gain scheduling of PID controllers, IEEE transactions on systems, man, and cybernetics, 23 (1993) 1392-1398.

[23] X. Gong, D. Cao, Fuzzy proportional-integral-derivative control of an overhang rotor with double discs based on the active tilting pad journal bearing, Journal of Vibration and Control, 19 (2013) 1487-1498.

[24] G. Li, B. Li, D. Wu, J. Du, G. Yang, Feedback linearization-based self-tuning fuzzy proportional integral derivative control for atmospheric pressure simulator, Proceedings of the Institution of Mechanical Engineers, Part I: Journal of Systems and Control Engineering, 228 (2014) 385-392.

[25] S. Azali, M. Sheikhan, Intelligent control of photovoltaic system using BPSO-GSA-optimized neural network and fuzzy-based PID for maximum power point tracking, Applied Intelligence, 44 (2016) 88-110.

[26] J. Kennedy, R. Eberhart, Particle swarm optimization, in: Proceedings of ICNN'95-International Conference on Neural Networks, IEEE, 1995, pp. 1942-1948.